Dokument ID	Version	Status	Reg. nr.	Sida
1395200	1.0	Godkänt		1 (22)
Författare Johan Öhman Niclas Bockgård			Datum 2013-05-16	
Kvalitetssäkrad av			Kvalitetssäkrad datum	
Godkänd av Sven Follin			Godkänd datum 2013-07-07	

TD05-Effects in ECPM translation

Contents

1 TD description

1.1 Context and approach

This document presents the hydrogeological modeling performed according to Task Description nr 5 (TD05) in SR-PSU (SKBdoc 1395344).

1.1.1 HRD realisations covering the variability range for SFR1 disposal facilities

As part of SDM-PSU, a HRD model has been developed for the SFR Regional domain (Öhman et al. 2012). The HRD model consists of unconditional stochastic realisations of connected discrete fracture networks (DFN) and conditioned Unresolved PDZs (conceptually modelled as connected to deformation zones of the Southern and Northern boundary belts. Bedrock heterogeneity causes uncertainty in model results (or, performance measures). Performance measures in SR-PSU, e.g. disposal facility flow (called cross flow), interactions between disposal facilities, and retention properties of the bedrock, must address the uncertainty range that is related to bedrock heterogeneity. Flow simulations are complex and time-demanding. Therefore, computational demand can be reduced if the "bedrock heterogeneity range" can be represented by a few characteristic HRD realisations, as inferred by means of statistical/geometric analysis of a larger ensemble of realisations.

1.1.2 ECPM conversion

Flow simulations in DarcyTools (Svensson et al. 2010) employ an Equivalent Continuous Porous Medium (ECPM) approximation of the hydraulic properties in the bedrock. The ECPM properties (e.g., Kx, Ky, Kz) are obtained by means of the inbuilt GEHYCO module, which uses a geometric method to upscale the hydraulic properties of an underlying fracture network. The target of the GEHYCO approach is to honour the fracture-network characteristics in a computational grid (for example: fracture size and fracture orientation leaving off prints as *grid cell anisotropy* and *directional correlation structures* in ECPM properties of the grid).
The shallow bedrock at the Forsmark-SFR site, as well as, in the surrounding Forsmark area is characterized as strongly horizontally anisotropic. It is therefore of interest to investigate how well the GEHYCO translation preserves hydraulic anisotropy.

The DFN-model calibration against borehole data (e.g., Öhman et al. 2012) includes large subsets of "small fractures" (i.e., fractures with radius down to borehole radius are included). For practical reasons, site-scale application (i.e., kilometre scale) typically requires a minimum fracture size truncation (i.e., only fractures above a certain side length are included in ECPM translation and subsequent flow modelling). In other words, the subset of small fractures, which is a component in the DFN borehole-calibration, is neglected in large-scale application. As the rule of thumb, it is recommended that the fracture side-length truncation is on par with the cell size (Svensson et al. 2010). Argumentations for this are that:

- Fracture size below cell size only raises the background conductivity, without contributing to correlation or anisotropy structures,
- Inclusion of small fractures is computationally demanding, and small fractures are to a lesser degree part of the globally connected system of flowing fractures
- ECPM conversion tends to hydraulically exaggeratet the geometric connectivity in rock mass. Exaggeration is partly reduced in a preceding step of removing isolated fractures (i.e., fractures not connected to the globally connected flowing fracture network). Small fractures are often envisaged as less transmissive and therefore less significant in the global flowing network. Thus, inclusion of numerous small fractures, of lower transmissivity, may reduce the efficiency in the isolated-fracture removal, and in turn, exaggerate ECPM hydraulic connectivity and smear the grid cell hydraulic anisotropy.

1.1.3 SFR1 and L1B

The layout of the existing SFR1 and the planned extension, version L1B (see SKBdoc 1395214 for more detail), is presented in Figure 1-.

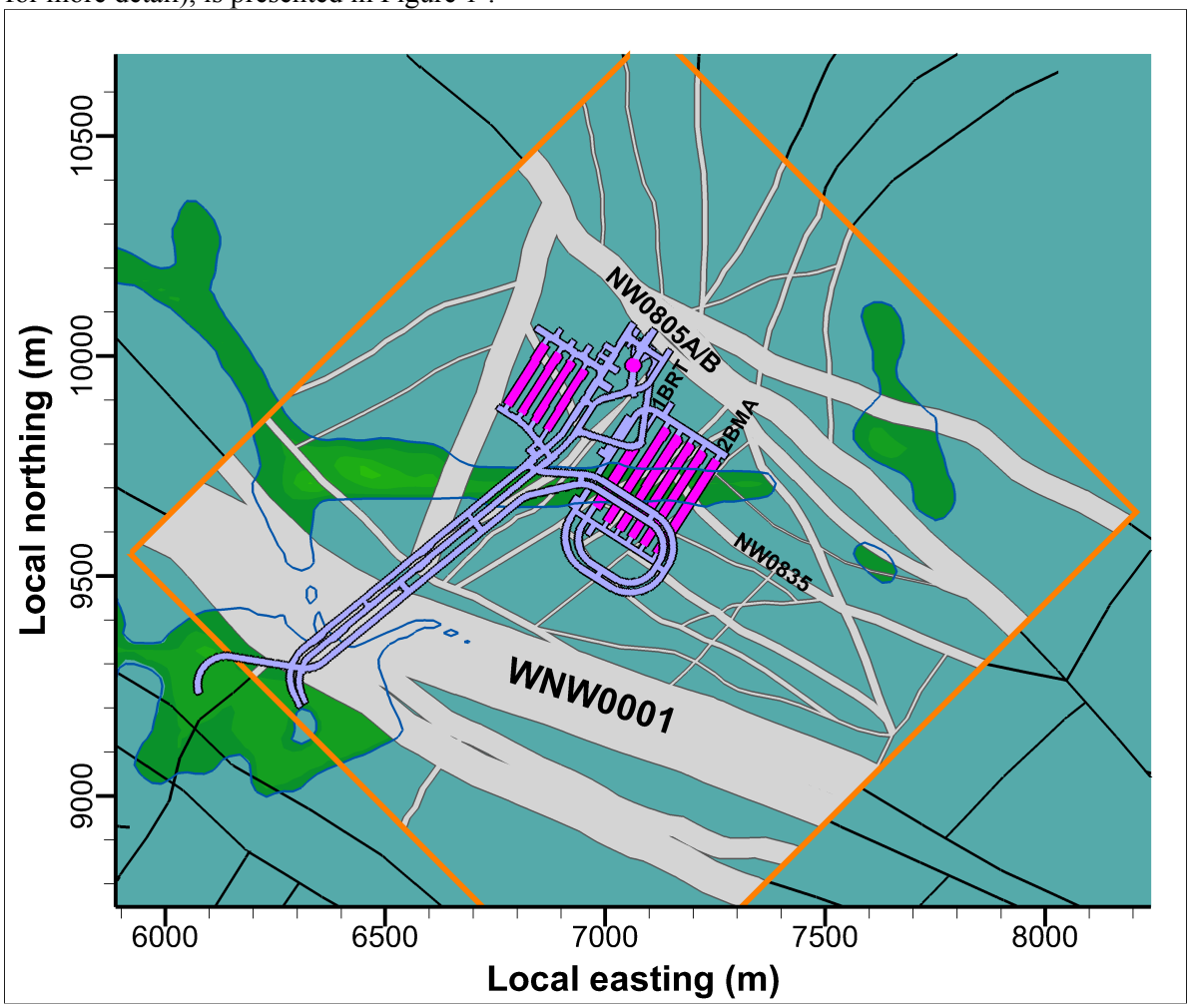

Figure 1-1 *Existing SFR1 and the planned extension, version L1B, in context of ground-surface intercepts of geologically modelled deformation zones (grey) and SFR Regional model domain (orange).*

1.2 Objectives

TD05 has the following three objectives:

- **Examine ECPM conversion**: The ECPM conductivity field resulting from a synthetic, anisotropic fracture network is examined in terms of the following properties: 1) anisotropy, 2) full range of conductivity values, and 3) correlation.
- **Determine DFN fracture-size threshold, L_{min}, for SR-PSU**: To identify suitable fracture-size thresholds, L_{min}, to provide realistic representation in ECPM properties in forthcoming SR-PSU Tasks.
- **Define representative HRD realisations for SFR1:** Out of 99 analysed HRD realisations, two are selected based on their geometric connectivity to represent the variability range for SFR1 disposal facilities. One is referred to as "optimistic" (characterised by few, low transmissive fractures intersecting the disposal facilities of SFR1) and one "pessimistic" (having the maximum number of fractures intersecting more than one disposal facility).

2 ECPM conversion of a synthetic horizontal fracture network

2.1 Methodology

A synthetic example is used to examine ECPM conversion of fracture-network characteristics. No site-specific geometric data are included in this synthetic study (i.e., tunnel geometry, deterministic geologic structures, ground surface topography, etc.). The computational grid is defined as an arbitrary cubic volume with side lengths equal to 200 m. This volume is discretised by cubic cells of side lengths 4 m (Figure 2-1). The 4 m cell size is judged to representative of the grid resolution of the SFR near-field in SR-PSU (i.e., ranging from 2 m tunnel cells to 8 m further away from tunnels).
Only fracture sets Hz and Gd of the Shallow and Repository depth domains are included in this study (parameterisation taken from Appendix 5 in SKB 2013). However, to accentuate anisotropy, the fracture set orientations are changed to strictly horizontal with negligible Fisher dispersion (i.e., high concentration) (CIF-command: **<lambda>** 0.0 0.0 -999. **</lambda>**). In other words, transmissivity and size is taken from the hydro-DFN model, whereas the orientation is modified to strictly horizontal.
The minimum fracture side length, L_{min}, was selected so as to correspond to a minimum transmissivity value of 10^{-8} m^2/s in the Shallow domain and 10^{-9} m^2/s in the Repository domain (Table 2-1). Large fractures (4 m < L < 300 m) are generated in a large volume surrounding the grid, while small fractures (4 m < L) are only generated inside the grid. Isolated fractures are **not** removed in this synthetic study.
The fracture network is then upscaled into grid ECPM conductivities by FracGen (the GEHYCO algorithm). Note that no deterministic structures are included.

Table 2-1. Size truncation of horizontal fractures

	Set	L_{min} (m)	r_{min} (m)	Log T (L_min)
Shallow domain	Hz	0.3	0.17	-8.0
	Gd	0.7	0.39	-8.1
Repository domain	Hz	1.2	0.68	-9.3
	Gd	0.4	0.23	-8.9

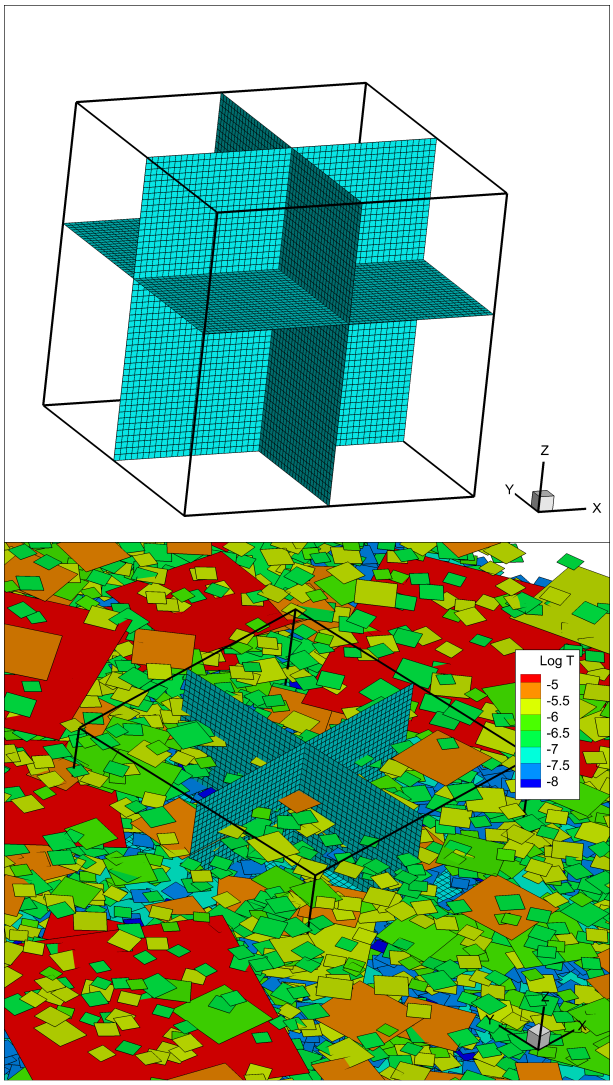

Figure 2-1. *Upscaling of synthetic fracture network. Left: grid with side lengths of 200 m, discretised by cells of side length 4 m. Right: synthetic horizontal fracture realisation (only L>10 m, z<-30m shown)*

2.2 Results

As expected, the synthetic, strictly horizontal fracture network renders strongly directional patterns in ECPM conductivity (i.e., directional correlation in conductivity, above cell scale). However, in spite of the relatively high grid discretisation, the ECPM conductivity is surprisingly well-connected for vertical flow (Figure 2-2). Results also demonstrate that ECPM translation of fracture network anisotropy at, or below cell scale is *not* preserved (Figure 2-3).

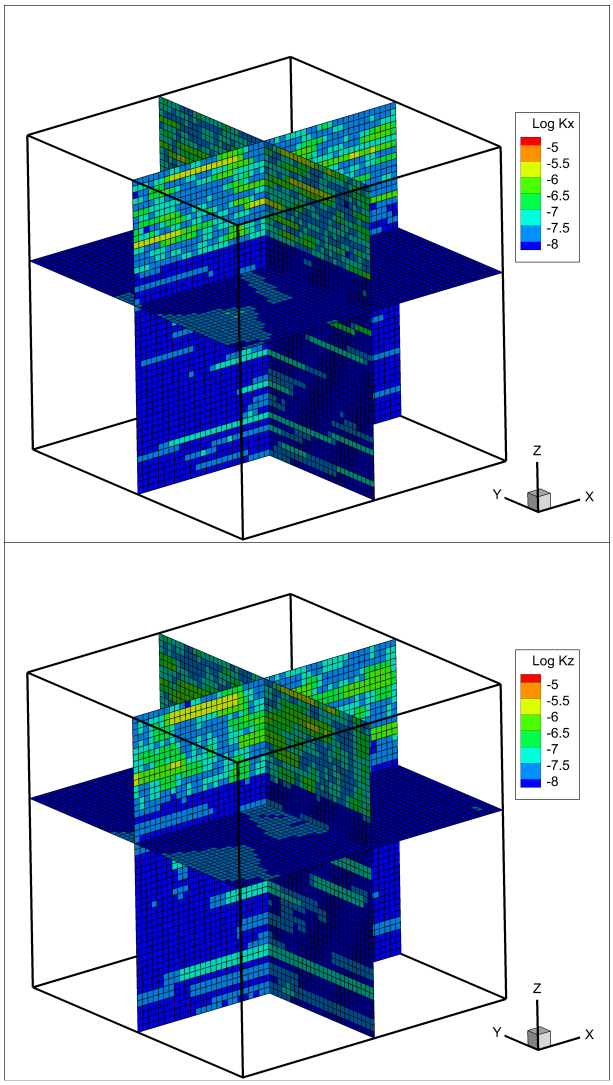

Figure 2-2. ECPM conductivity of a synthetic, strictly horizontal fracture network, in x and z directions.

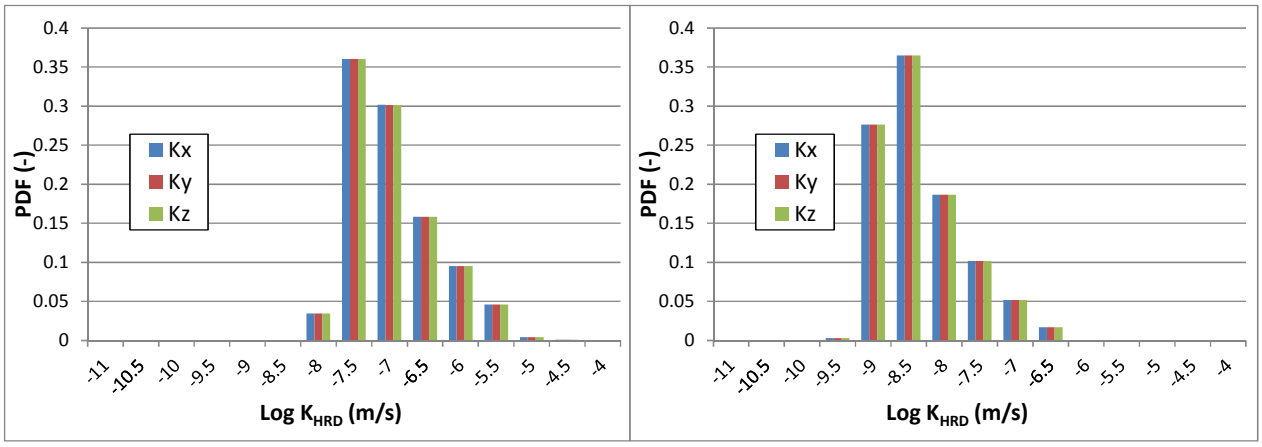

Figure 2-3. *No global anisotropy is identified between K_x, K_y, K_z distributions; neither in Shallow, nor Repository domains.*

Although the correlation of conductivity above cell scale, arising from large structures, is well-represented, the *lack of vertical connectivity* in the underlying fracture network cannot be resolved for the studied grid resolution (cell size 4m), at least not in the Shallow domain. To resolve the lack of vertical connectivity, the cell size must be smaller than the separation

distance between the horizontal fractures. In other words, inclusion of too small fractures leads to an overestimation of connectivity in the ECPM property fields.

3 Effect of size truncation in large-scale DFN applications

3.1 Methodology

Role of fracture size in calibration

Fracture size is the most uncertain parameter in the DFN model. Unless support is available from exposed rock surfaces (outcrops or tunnel walls), it must be inferred from calibration to borehole data. The hydro-DFN model SFR v. 1.0 (Öhman et al. 2012) was calibrated by means of a Connectivity analysis, in which the fracture size distribution is inferred from the ratio between the total population of fractures mapped as open and its subset of hydraulically connected fractures. The two most important assumptions in this method are: 1) fracture transmissivity, as measured by the PFL-logging device, is proportional to fracture size (radius of circular fracture or side length of square fracture), and 2) the radius of smallest fracture in the borehole data sample, r_0, is equal to borehole radius, $r_{bh} = 0.038$ m. Due to computational demand, small fractures cannot be generated over large volumes. Therefore, a particular procedure is undertaken in the calibration process, in which large fractures are generated over a large domain to establish global connectivity, while small fractures (down to borehole radius) are only generated in the vicinity of the sampling boreholes. The size distribution of open fractures is calibrated by reproducing the subset of hydraulically active, or globally connected, fractures observed in data.

Truncation of small fractures in large-scale application

Due to the nature of power-law scaling fractures, inclusion of ever smaller fractures imply drastically increasing computational demand (see number of fractures in Table 3-1). Limitations in computational capacity necessitate a truncation of the smallest fractures, L_{min}. Size truncation is motivated by the fact that small fractures have a less pronounced role in the ECPM conductivity field: 1) small fractures are assumed to have lower transmissivity, 2) fracture sizes below grid resolution (cell size) provide no additional correlation to the ECPM conductivity field, and 3) less connected (even large amounts of generated features provide little additional connected fracture intensity, $P_{32,\,COF}$).
The impact of truncating small fractures is evaluated in terms of ECPM properties to demonstrate the representation of the hydraulic connectivity/conductivity in large-scale flow applications. Should the results of truncation be unrealistic, the neglected fracture properties (transmissivity, porosity, and flow-wetted surface area) can be superimposed on to the ECPM properties in post-processing (i.e., the spatial correlation/anisotropy of fracture properties below grid resolution cannot be resolved in the computational grid, and can therefore be efficiently handled outside the GEHYCO module).

Analysis of fracture-size truncation, in terms of ECPM properties

The ECPM translation of the hydro-DFN model SFR v. 1.0 is examined for three size classes, with the purpose is to identify a suitable minimum fracture size, L_{min}, for application in SR-PSU. Three fracture-size classes are defined, based on fracture side length, L:

- **Small**: fractures **below** cell size, defined as $L_{min} < L \leq 4$ m (L_{min} defined in Table 3-1)
- **Medium**: fracture sizes that are similar to cell size, defined as 4 m < L ≤ 8 m
- **Large**: fractures **exceeding** cell size, defined as 8 m < L ≤ 300 m

Similar to the study of synthetic data (Section 3.1), the minimum fracture side length, L_{min}, was selected so as to correspond to a minimum transmissivity value of 10^{-8} m^2/s in the Shallow domain and 10^{-9} m^2/s in the Repository domain (Table 3-1). The grid resolution is 4 m and covers a 200 × 200 × 200 m^3 volume located near the existing SFR1 (i.e., the Shallow and Repository domains are represented).

Table 3-1. Ranges of generated fracture sizes and transmissivity

	Number of fractures[1)]	log T_{min}[1)]	log T_{max}

Domain	Set	L_{min} (m)	Small	Med	Large	Small	Med	Large	L = 300 m
Shallow	EW	1	96,703	995	2074	-8.0	-7.2	-6.8	-4.8
	NW	0.5	382,897	451	963	-8.0	-6.8	-6.4	-4.6[2)]
	NE	0.7	108,203	243	417	-8.1	-7.4	-7.1	-5.5
	Gd	0.7	460,830	3,241	9,351	-8.1	-7.3	-7.0	-5.2
	Hz	0.3	2,892,842	2,996	9,998	-8.0	-6.5	-6.1	-4.6[2)]
Repository	EW	0.7	493,571	2,121	2,655	-9.1	-8.3	-8.0	-6.2
	NW	0.4	1,784,166	1,614	2,384	-8.7	-7.6	-7.2	-5.6[2)]
	NE	0.7	238,641	703	811	-9.2	-8.2	-7.8	-5.8
	Gd	0.4	3,482,641	5,647	10,378	-8.9	-8.1	-7.9	-6.6
	Hz	1.2	177,310	7,463	15,301	-9.3	-8.6	-8.2	-6.1
Deep	EW	4		72	460		-7.9	-7.4	-6.5[2)]
	NW	4		64	359		-7.9	-7.6	-6.5[2)]
	NE	4		73	444		-8.4	-8.1	-6.5
	Gd	4		590	4,887		-9.0	-8.5	-6.5[2)]
	Hz	4		249	2,035		-8.3	-8.0	-6.5[2)]

1) Small defined as $L_{min} < L \leq 4$ m, Medium defined as 4 m < L ≤ 8 m, Large defined as 8 m < L ≤ 300 m
2) Maximum transmissivity constrained by field data

Removal of isolated fractures:

The following structures are included as geometric boundaries for hydraulic connectivity:

- Deformation zones inside the studied sub-volume (only ZFM871, ZFMNW0805A/B)
- SBA structures inside the studied sub-volume (only SBA7)
- Unresolved PDZs (Unresolved_PDZ_R01_knwn, none inside the selected volume)
- Existing SFR1 (rock caverns partly inside the selected volume)
- Planned extension L1B (entirely outside the selected volume)

These geometries contribute to *connectivity* alone; ECPM values reflect *only* stochastic fractures. The impact of truncating small fractures in ECPM translation (e.g., Figure 3-1) is quantified for three cases and related to available PFL data:

1) ECPM conductivity of Large fractures
2) ECPM conductivity of Medium to Large fractures
3) ECPM conductivity of All fractures exceeding L_{min} (as defined from T_{min} in Table 3-1)

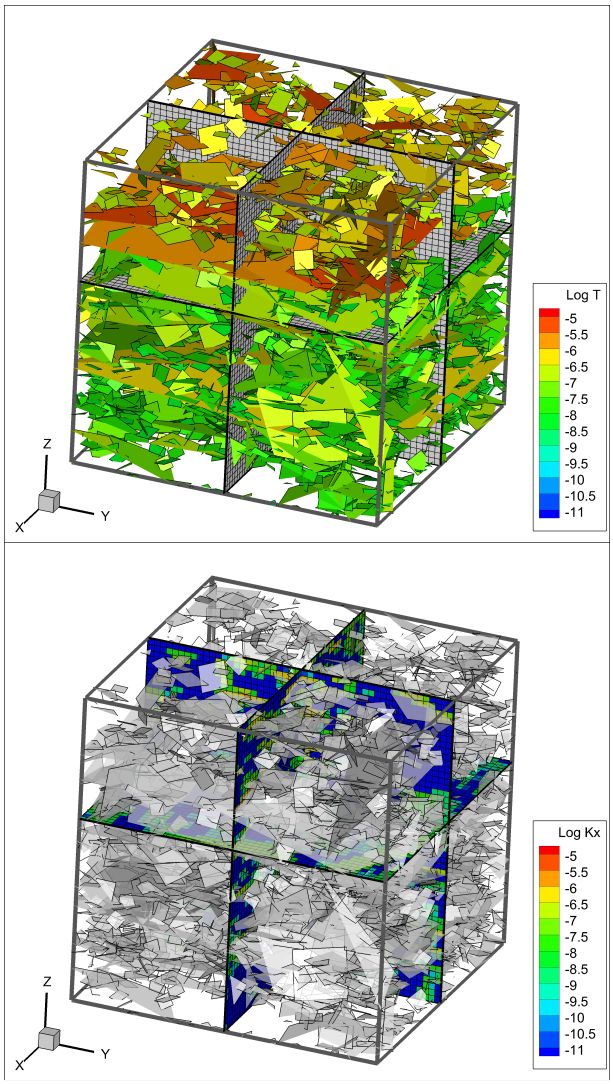

Figure 3-1. *ECPM translation of large fractures (L > 8 m). Left: stochastic fractures and computational grid, right: corresponding ECPM conductivity.*

3.2 Results

The impact of truncating small fractures in ECPM translation is quantified for three cases:

1) ECPM conductivity of large fractures
2) ECPM conductivity of medium to large fractures
3) ECPM conductivity of all fractures exceeding L_{min} (as defined from T_{min} in Table 3-1).

In a second step, the resulting ECPM conductivity is related to available PFL data.
It should be emphasized that the results are derived from a single DFN realization, and for the particular settings surrounding the local volume. It should also be noted that the sample size in underlying PFL data for the Shallow domain DFN model is small. Excluded data of the Shallow domain are predominantly low-transmissive, causing large uncertainty to the lower tail of transmissivity in the Shallow domain. The Repository domain is supported by a considerably higher data sample.

ECPM conductivity patterns with fracture-size truncation

The large fractures are common in all three cases and constitute the hydraulic backbone, or the large-scale correlation structures, in the ECPM conductivity field (Figure 3-2a,b). The ECPM grid for large fractures has the distinct characteristics of a sparsely fractured bedrock with a highly channelized fracture network and compartmentalised rock volumes located in between. Inclusion of medium-size fractures smears out these characteristics (Figure 3-2c,d); the hydraulically connected pathways are widened and the compartmentalised areas are reduced.

Inclusion of the small fractures adds on a background conductivity of c. 10^{-8} to 10^{-7} m/s in the Shallow domain, and 10^{-9} to 10^{-8} m/s in the Repository domain, almost completely eliminates the isolated rock volumes (Figure 3-2e,f). The hydraulic backbone of large fractures still remains as high-transmissive channels; notably, their ECPM conductivity is also increased by the inclusion of small fractures.

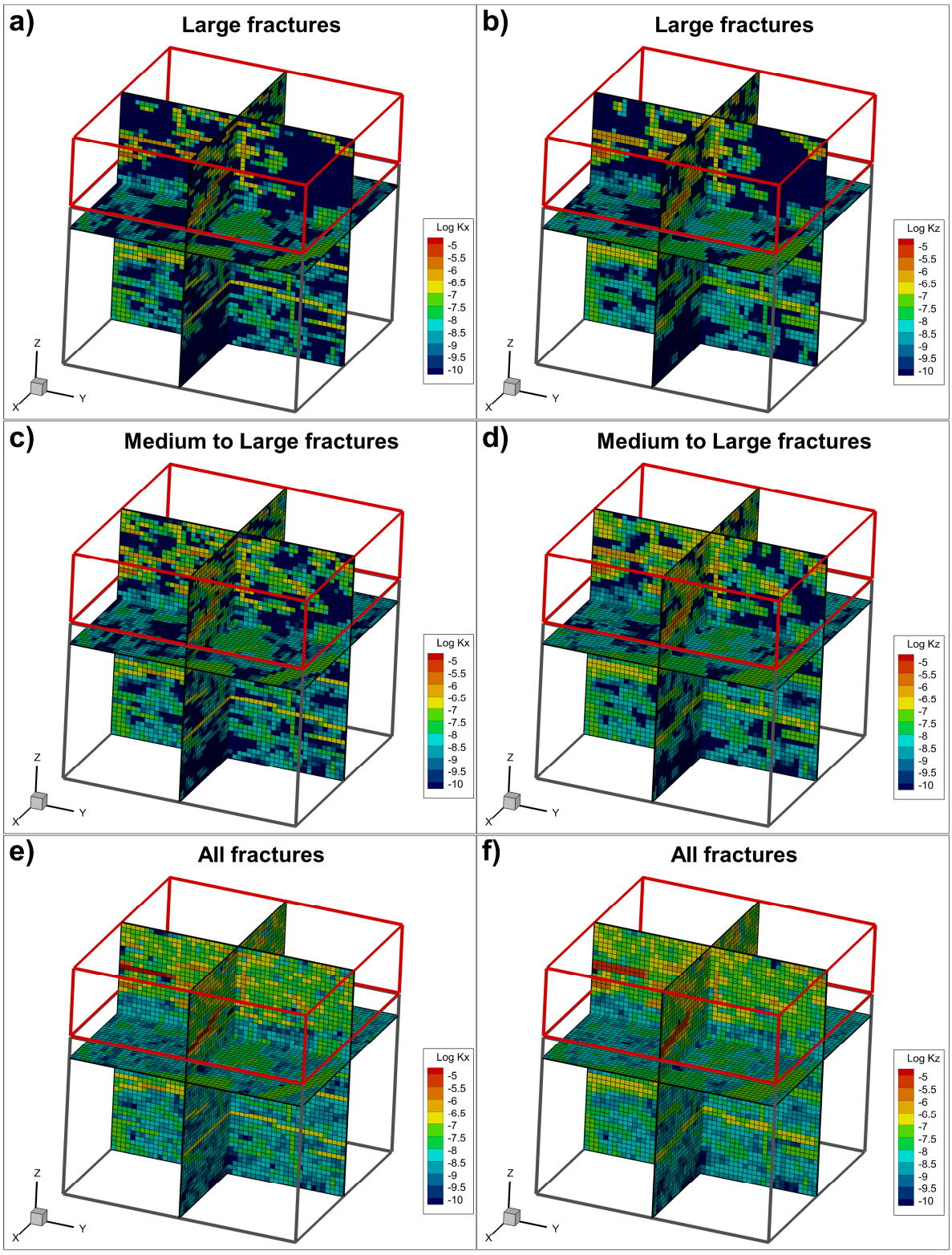

Figure 3-2. *Resulting ECPM conductivity fields (Kx and Kz) of the three cases of fracture size range included. Large fractures control large-scale correlation pattern, Small fractures control the background conductivity.*

ECPM conductivity and PFL data

Small fractures have a significant contribution to the lower tail of ECPM conductivity distributions (Figure 3-3c and d). In comparison to data, exclusion of small fractures provides an excessive proportion of zero-ECPM conductivity (shown as log K = -10.5 in Figure 3-3).

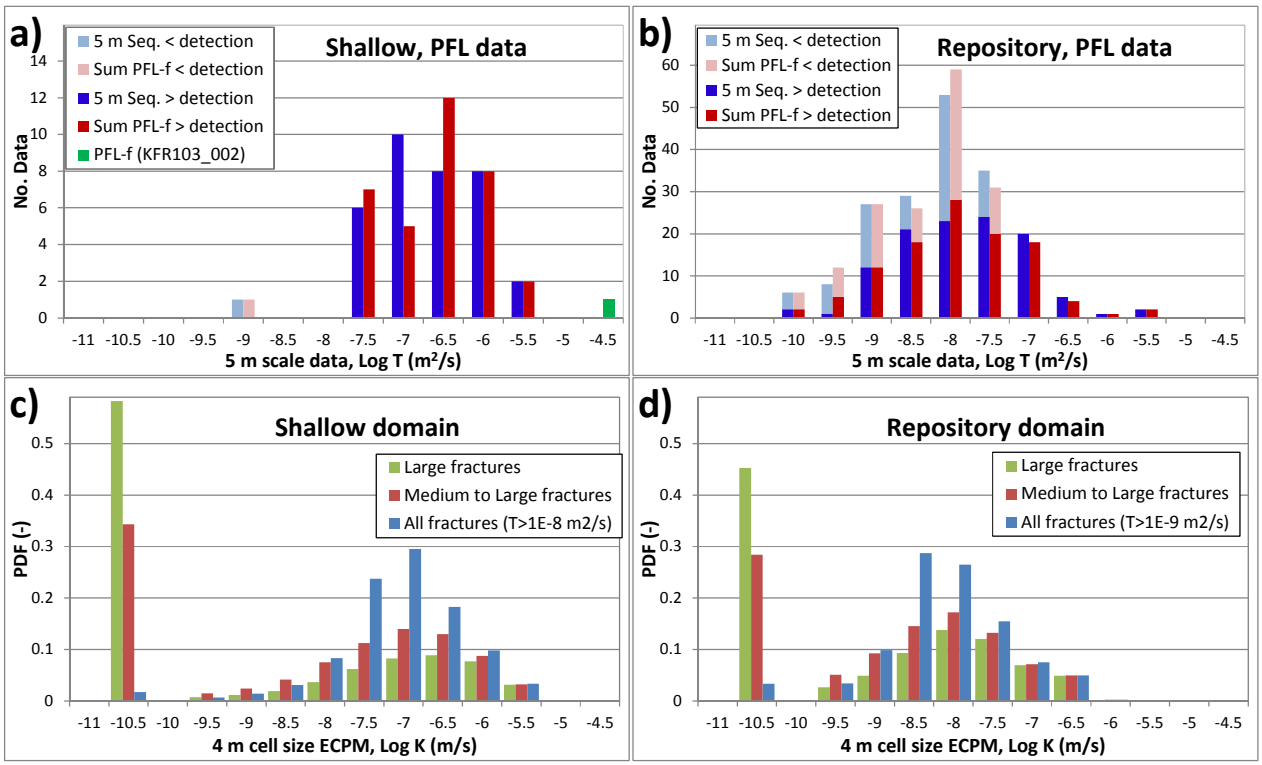

Figure 3-3. *PFL transmissivity (5 m scale) and translated ECPM conductivity (4 m scale) for Shallow and Repository domains. Sequential 5 m PFL data compared to sum of PFL-f transmissivity inside intervals. Five-meter sections below detection limit are shown in pale colours. Deformation zones, SBAs, and Unresolved PDZs are excluded from data. The difference between conductivity and transmissivity at the 4-5 m scale is almost equivalent of one logarithmic bin (i.e., log(4) ≈ 0.6). The most transmissive PFL-f, KFR103_002, is not covered by 5 m sequential PFL data. Zero ECPM conductivities represented in the logarithmic bin -10.5.*

However, the lower tails in data distributions are subject to uncertainty and open to alternative interpretations. In the Shallow domain, the uncertainty relates to the small sample size available; the fraction of records below detection limit depends on which data set is used. In the PFL data used in the DFN calibration, only one interval out of 34 (1/34 = 3%) are below detection limit, log T_{lim} = -9. The fraction of data below detection limit is best matched by including the small fractures (blue bars in Figure 3-3c). It should be noted that the sample size of PFL-logged 5 m intervals is small in the Shallow domain. If additional data from KFR27 and KFR106 are included, 7/47 = 15% are below detection limit. Owing to data scarcity, the historic data set can provide additional information, in spite of its poorer detection limit and quality. The historic data set involves different test methods and scales, but "typically" consists of 3 m short-term packer tests with detection limit on the order 5×10^{-8} m^2/s. Adjacent packer data can be combined to estimate the number of data below detection limit at the 6 and 9 m scale (Table 3-2).

Table 3-2. Data below detection limit in the Shallow domain

Data set	Type	Scale	Log T_{lim}	No. below det.	Percentage
Recent data, DFN data	PFL sequential	5 m	-9	1/34	3%
Recent data, All PFL data	PFL sequential	5 m	-9 to -7.5	7/47	15%
Historic data, non-modified	Short-term packer	3 m	-8.2 to -7.1	118/229	52%
Historic data, sum. intervals	Short-term packer	6 m	-8.2 to -7.3	38/104	37%
Historic data, sum. intervals	Short-term packer	9 m	-7.3	22/78	28%

The historic data provide a very different criterion for "fraction of data below detection limit", indicating that "medium to large" fractures are sufficient to reproduce data (c. 30 to 40% below log T_{lim} = -7.3; orange bars Figure 3-3c).

The Repository domain is supported by a considerably larger sample from the recent data set; hence, historic data provides less additional value. The uncertainty in the lower tail of the Repository domain relates to the wide range of detection limits and the numerous data falling below detection limit. The PFL data set has 40% below detection; the detection limits range from Log T_{min} = -10 to -7.5. Two endpoint assumptions for the data below detection limit can be identified:

1. they reflect more or less impermeable rock (i.e., log T = -10), or
2. they follow the overall data pattern (i.e., just barely falling below detection limit, $T \approx T_{min}$).

The "medium to large fractures" are sufficient for ECPM translation in case 1 (orange bars in Figure 3-3d), while the contribution of small fractures in ECPM translation is required for case 2 (blue bars in Figure 3-3d).

In summary, the fracture size range exceeding cell size 4 m (referred to as "medium to large fractures") control the hydraulic connectivity/large-scale correlation structures and reasonably well reproduce the upper tail of ECPM conductivity. The compartmentalised regions, arising from excluding small fractures, are in line with the conceptual understanding of the site, as well as, experience of the existing SFR. One disadvantage of including small fractures is the excessive vertical connectivity in the system (Figure 2-2; Figure 3-2f). The uncertainty in lower tails of transmissivity/conductivity opens to alternative data interpretations, leading to a discussion on what is considered to be "conservative" in SR-PSU:

- Exclusion of small fractures leads to shorter travel time and lower F-quotients (as less kinematic porosity and flow-wetted surface area is included; Figure 3-5 and Figure 3-6)
- Inclusion of small fractures increases ECPM conductivity and connectivity, leading to higher flows in in simulations (e.g., total disposal-facility flow and number of possible flow paths across disposal facilities). Without a revision of anisotropy in the GEHYCO algorithm to account for fracture geometry versus the grid (suggested in Section 5.1), inclusion of small fractures imply a risk of unrealistic connectivity. Alternatively, derived ECPM properties of small fractures in this study could be superimposed onto the *horizontal* conductivity components, K_{xy}, in post-processing (e.g., PropGen). This could be made by defining a PDF related to fractures below cell-size (difference between orange and blue bars in Figure 3-3c,d). In other words, the vertical conductivity field would have the appearance of Figure 3-2b, while the horizontal conductivity would have the appearance of Figure 3-2c.

All results represent a single realisation, for a local grid with specific cell-size resolution and a specific location within the SFR Regional domain (i.e., with respect to connectivity). Small-fracture contribution of ECPM porosity, FWS, and horizontal conductivity are shown relative to the "hydraulic backbone" (ECPM properties of fractures larger than cell-size; Figure 3-5 and Figure 3-8).

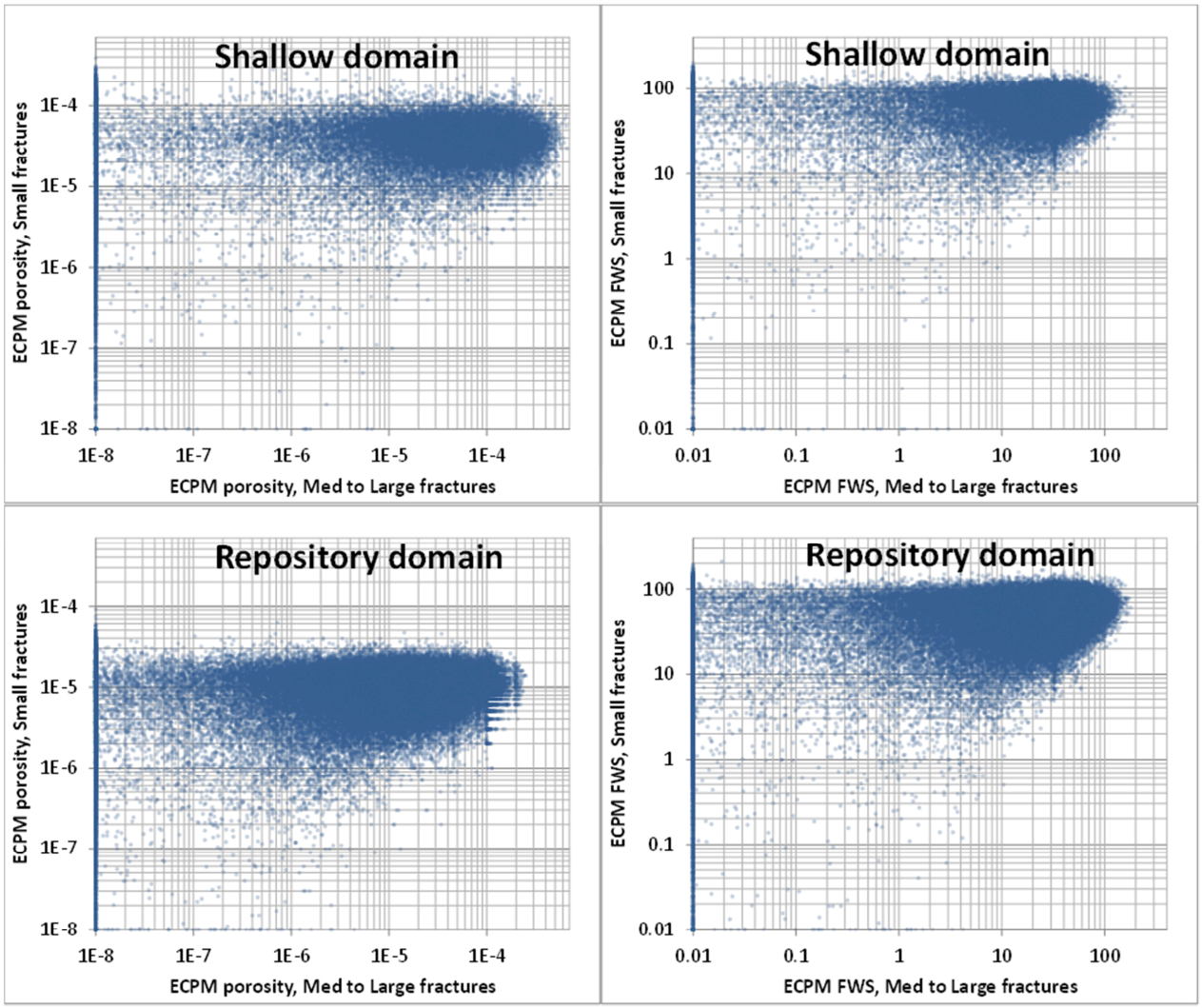

Figure 3-4. *ECPM property cross plot between size ranges; above cell size (medium to large fractures) and below cell size (small fractures). FWS has the unit (m^2/m^3).*

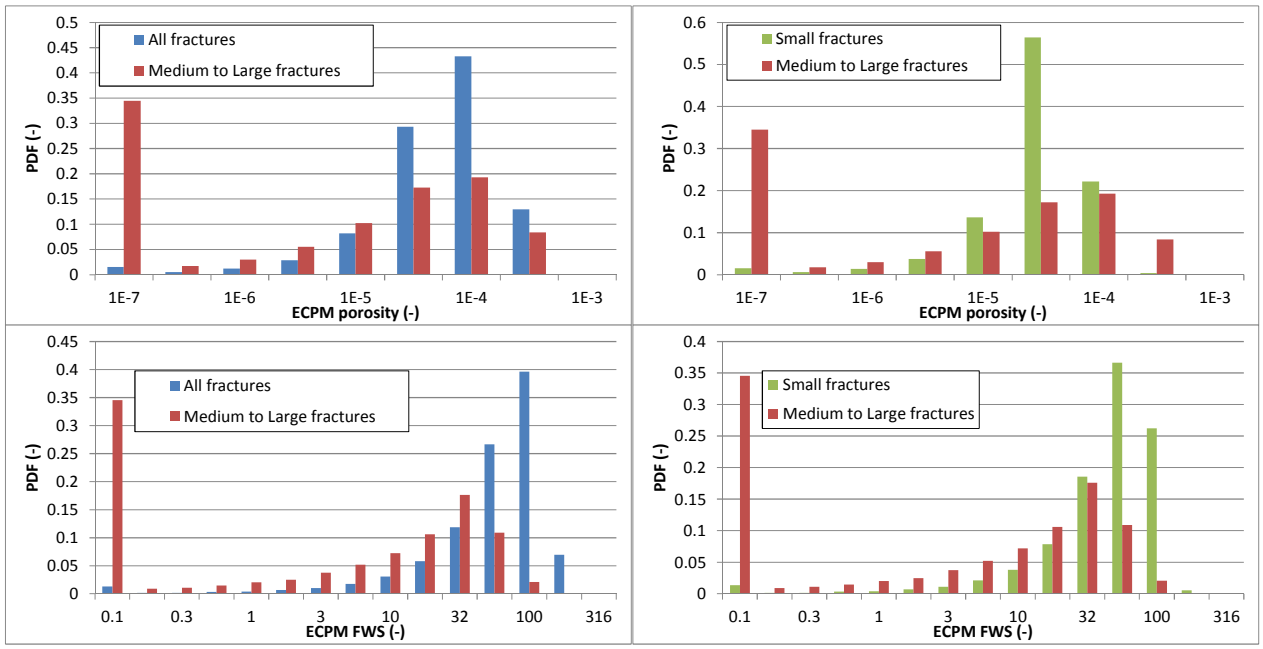

Figure 3-5. *ECPM Porosity and FWS for different size ranges in Shallow domain. FWS has the unit (m^2/m^3).*

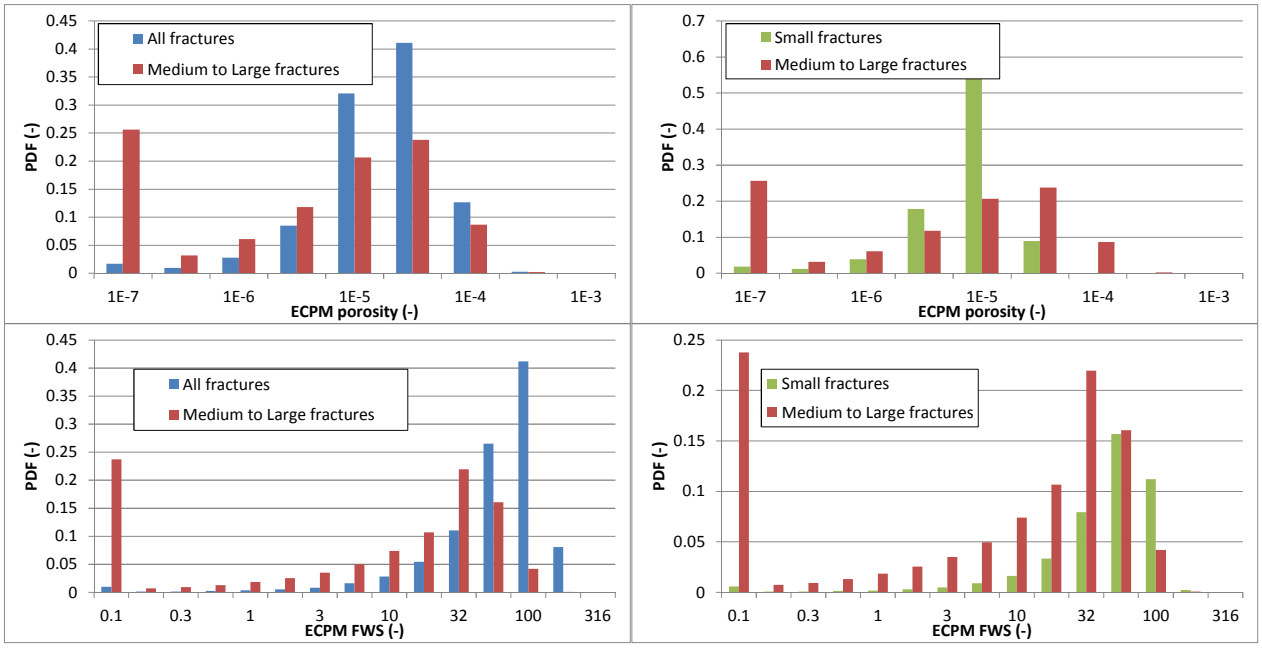

Figure 3-6. *ECPM Porosity and FWS for different size ranges in Repository domain. FWS has the unit (m^2/m^3).*

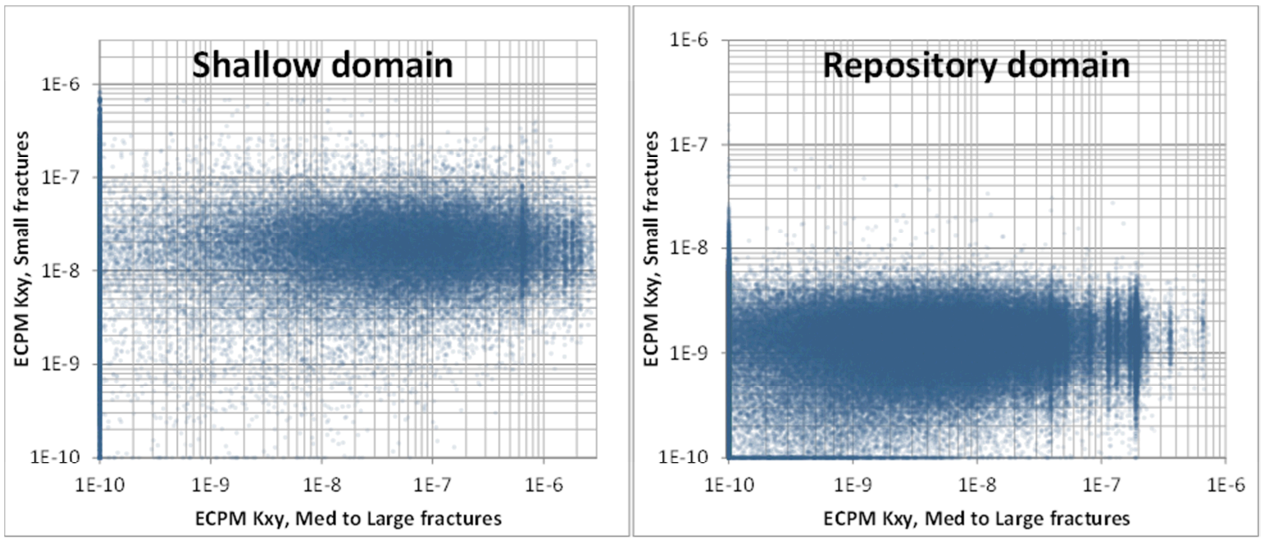

Figure 3-7. *ECPM K_{xy} cross plot between size ranges; above cell size (medium to large fractures) and below cell size (small fractures).*

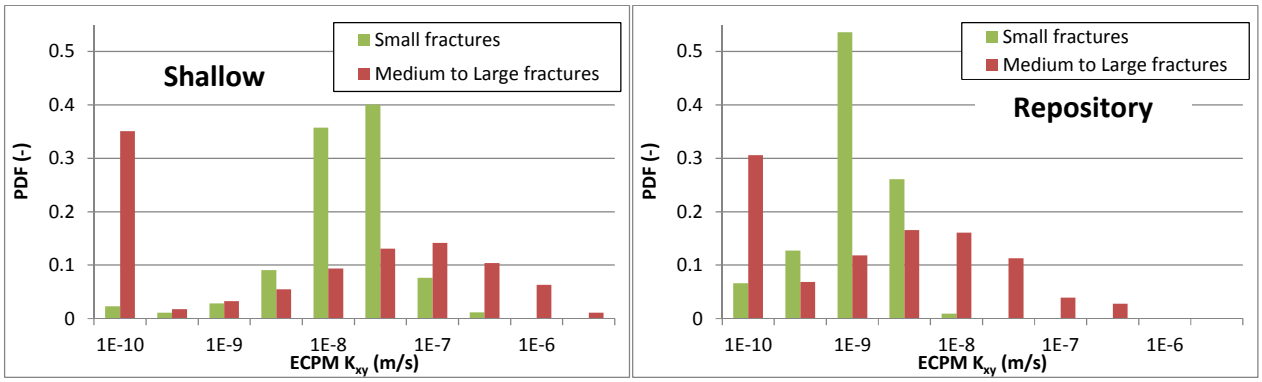

Figure 3-8. *ECPM K_{xy} distributions for size ranges above cell size (medium to large fractures) and below cell size (small fractures).*

4 Statistical analysis of 99 HRD realisations

4.1 Methodology

An ensemble of stochastic realisations, R01 to R99, of connected fracture networks and Unresolved PDZs are generated (Table 4-1). The DFN parameterisation is taken from Appendix 5 in SKB 2013. Based on the analysis of ECPM conversion, the fracture-size truncation, L_{min} is 4 m in the Shallow and Repository depth domains, and 16 m in the Deep depth domain.

Table 4-1. Execution sequence in generation and analysis of HRD realisations

Purpose, [code], [input]	[output] Description
Construct input file for DarcyTools fracture generation, [Sample_DFN.F90], [DFN_input_template.dat]	[cif.xml] standard DarcyTools Compact Input Command file for fracture network generation according to DFN model parameterisation (Appendix 5 in SKB 2013). Seed = **XX**×10^{-4}.
Generate stochastic realisation **XX**, within region exceeding SFR Regional domain by at least L_{max} = 300 m, DarcyTools module [FracGen], [cif.xml]	[All_domain_Frax] temporary fracture file (DarcyTools "random-fracture format")
Exclude all fractures with centre coordinate outside the SFR Regional domain, [Exclude_Frax_outside_SFR_Reg_dom.f], [All_domain_Frax]	[All_FRAX_in_SFR_DOMAIN] reduced, temporary fracture file (DarcyTools "random-fracture format")
Construct input file for subsequent isolated-fracture removal [Exclude_Frax_outside_SFR_Reg_dom.f]	[cif.xml] standard DarcyTools Compact Input Command file for isolated fracture removal. Geometrical data defining the connected fracture network specified in Table 4-2.
Remove isolated fractures, DarcyTools module [FracGen], [cif.xml], [All_FRAX_in_SFR_DOMAIN]	[Connected_DFN.DT] temporary file with connected fracture network (DarcyTools "random-fracture format")
Read, trim, and sample connected fractures intersecting disposal facilities in SFR1 and L1B[2)] [Sample_DFN.F90] [Connected_DFN.DT] [Unresolved_PDZ_R**XX**_knwn]	Transmissivity trimming, based on lowest fracture corner, z_{min}: z_{min} < -60 m ➔ $T_{max} = 10^{-5.6}$ m^2/s z_{min} < -200 m ➔ $T_{max} = 10^{-6.5}$ m^2/s
[SFR-1_Tunnel_geometry.dat], [SFR-1_Disposal_geometry.dat] [SFR-2_Tunnel_geometry.dat] [SFR-2_Disposal_geometry.dat] Export rotated DFN realisation and rotated Unresolved PDZ realisation [Sample_DFN.F90]	Sampling thresholds: T_{min} >10^{-6} m^2/s for tunnels, T_{min} >10^{-7} m^2/s for disposal facilities [Tunnel_intersections.dat] Sampling statistics [Exported_fracts_R**XX**.plt] TecPlot file [R_SFR_DFN_connected_R**XX**_knwn] [R_Unresolved_PDZ_R**XX**_knwn] (rotated DarcyTools "known-fracture format")

3) **XX** = realization 01 to 99
4) L1B geometries are labeled "SFR-2"

Table 4-2. Deterministic geometries defining bounds in the isolated-fracture removal

Files	Description
Parameterized_SFR_HCD	Deformation-zone geometery
Parameterized_SFR_SBA1_to_SBA8	Deterministic SBA-structure geometry
SERCO_DFN_WITH_HOLE	Deterministic DFN outside the SFR Regional domain. Truncated version, excluding fractures located more than 300 m outside SFR Regional domain
Unresolved_PDZ_R**XX**_knwn	Corresponding Unresolved PDZ realisation (**XX** = 01 to 99).
EXISTING_SFR_knwnf	Tunnel geometry of the existing SFR1 in "known-fracture format".
ENTIRE_L1_z117_knwnf	Tunnel geometry of the extension in "known-fracture format", constructed from TecPlot files by means of [Convert_TEC_to_knwnf.f].

Geometric intersections between fractures tunnels/disposal facilities of SFR1 and L1B are sampled and the statistics is exported in an ASCII output file. Based on the statistics of intersections in SFR1 disposal facilities, two realisations are selected to represent of the range of variability in the ensemble: a "pessimistic" and an "optimistic" realisation.
The measure chosen for the ranking of the realisations was the number of fractures intersecting more than one tunnel in the existing SFR facility. All parts of the facility were included in the analysis, but only fractures with T > 1·10–7 m/s and T > 1·10–6 m/s were accounted for in the repository caverns and in other tunnels, respectively. This measure was believed to reflect the "danger" of the realisation since hydraulic connections between different repository parts are undesirable and since there is a correlation between fracture size (large fractures more likely to intersect several repository parts) and fracture transmissivity. This measure was also found to be quite decisive, making it possible to discriminate between different realisations.

4.2 Results

In total 99 realisations were generated. There are no Unresolved PDZs intersecting the existing rock vaults. The median of the number of fractures intersecting more than one tunnel in the existing SFR facility was 3 fractures (Figure 4-1). The range in the number of fractures intersecting more than one tunnel per realisation was from zero up to seven (Figure 4-2). There were six realisation with no fracture intersecting more than one tunnel and two realisations with seven fractures intersecting more than one tunnel.

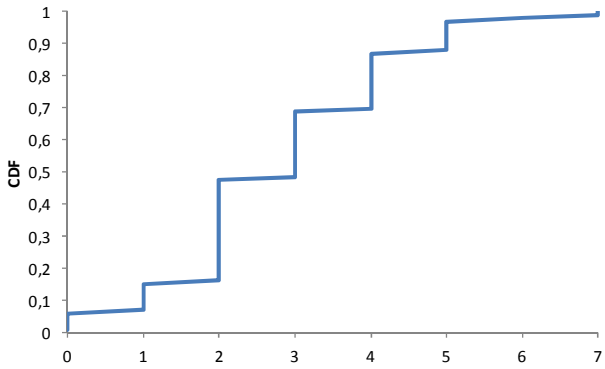

Figure 4-1. *CDF of the number of fractures intersecting more than one tunnel in the existing SFR facility.*

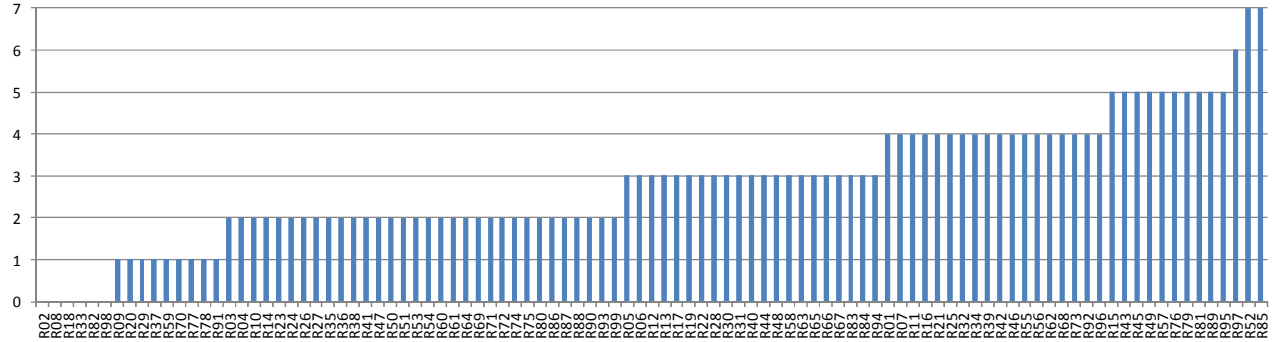

Figure 4-2. *Realisations ranked by number of fractures intersecting more than one tunnel in the existing SFR facility*

Of the six realisations with no fracture intersecting more than one tunnel, realisation R18 was chosen as the optimistic case and of the two realisations with seven fractures, realisation R85 was chosen as the pessimistic case. R18 and R85 were chosen since they were the realisations with the lowest and highest number of fractures intersecting more than one tunnel when both the existing SFR facility and the proposed layout of the extension were taken into account (Figure 4-3). The two chosen realisations were also among the realisations with the lowest and highest

total number of tunnel intersections and the lowest and highest summed transmissivity of intersecting fractures, respectively (Figure 4-4 and Figure 4-5). Realisation R85 was actually ranked highest by all these measures. The probability for the chosen realisations can be estimated from the empirical CDF (Figure 4-1), where the probability of zero fractures is about 6% and the probability of seven or more fractures is about 1% only.

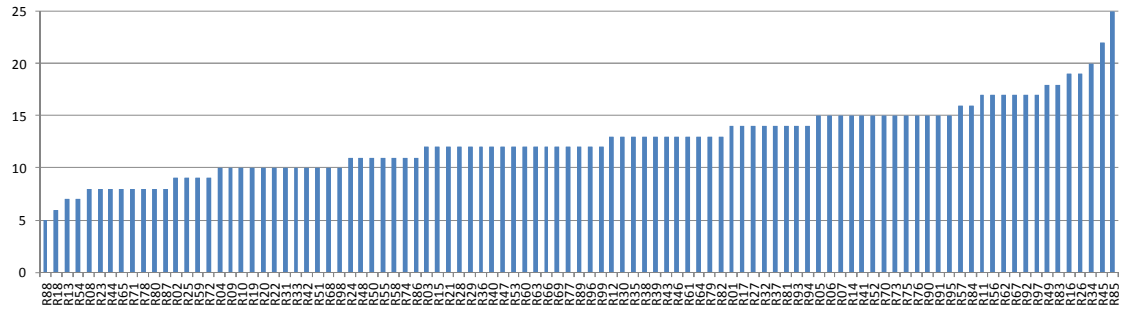

Figure 4-3. *Realisations ranked by number of fractures intersecting more than one tunnel in the existing SFR facility or the proposed layout of the extension.*

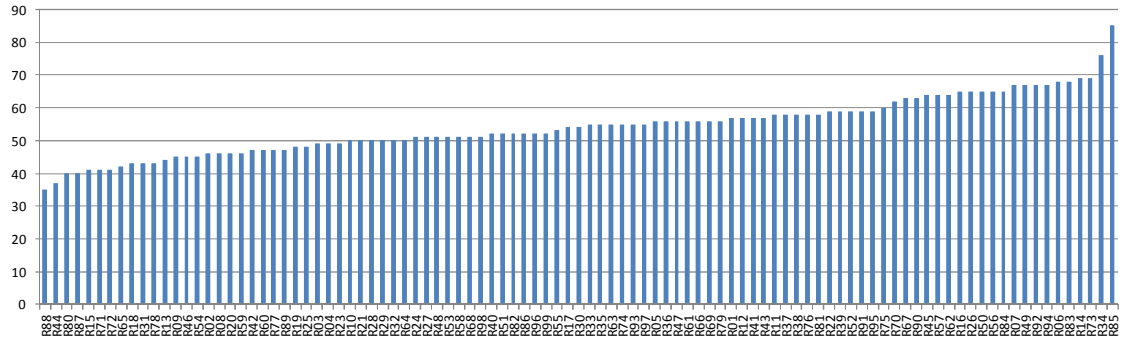

Figure 4-4. *Realisations ranked by total number of intersections between DFN fractures and the existing SFR facility or the proposed layout of the extension.*

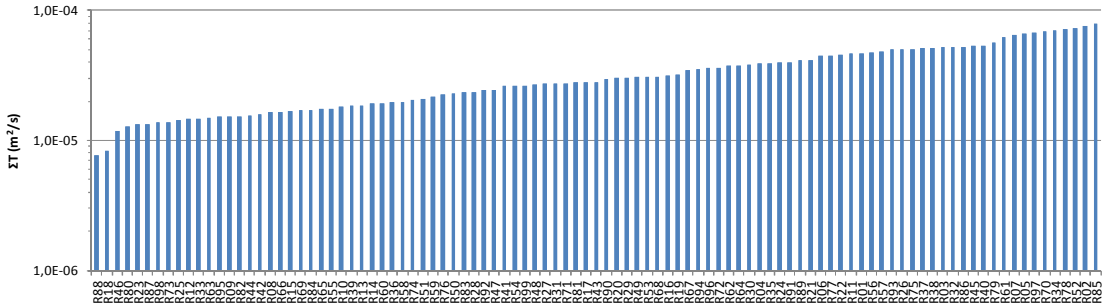

Figure 4-5. *Realisations ranked by summed transmissivity of fractures intersecting the existing SFR facility or the proposed layout of the extension.*

5 Recommendations

5.1 ECPM conversion

Inclusion of unnecessarily small fractures below cell size should be circumvented to reduce an exaggerated hydraulic connectivity in the ECPM property grid.
The GEHYCO algorithm should be revised to better represent hydraulic anisotropy. On proposal is to include consideration to directional cosines of fractures inside cells similar to the Oda permeability-tensor concept. In other words, let the contribution of fracture properties to the intersected cell-wall control volume be determined by the scalar product between the fracture plane and the normal of the cell wall. For example, this would provide ECPM $K_z = 0$ for the tested, synthetic fracture network.

5.2 Fracture size truncation in large-scale DFN applications

It is recommended that the following size truncation, L_{min}, are applied in DFN realisations for SR-PSU:

- L_{min} = 4 m for z ≥ -200 m (i.e., Medium to Large fractures inside the Shallow and Repository domains, where grid discretisation ranges in cell-size from 8 to 2 m), and
- L_{min} = 16 m for z < -200 m (i.e., Deep domain, where grid discretisation ranges in cell-size from 16 to 32 m).

Should these truncations be considered non-conservative in SR-PSU, for example in calculation of disposal-facility flow, an *alternative* approach could be to superimpose the contribution of small fractures to the *horizontal* components in ECPM conductivity (i.e., green bars in Figure 3-8) as a post-processing step.

5.3 Representative HRD realisations for SR-PSU

Based on statistics of fractures intersecting SFR1 disposal facilities, two HRD realisations are selected to represent the variability range in SR-PSU:

- R18 is selected as an “optimistic” realisation
- R85 is selected as a “pessimistic” realisation

Realisations R01 to R20, and R85 are stored for application in subsequent SR-PSU Tasks (e.g., TD08). Note that that the connectivity in these realisations is valid for the coexistence of SFR1 and L1B. Updated geometries in the layout of the planned SFR extension may imply that the HRD realisations must be re-generated.

6 References

SKB, 2013. Site description of the SFR area at Forsmark at completion of the site investigation phase, SDM-PSU Forsmark. SKB TR-11-04, Svensk Kärnbränslehantering AB.

Svensson U, Ferry M, Kuylenstierna H-O, 2010. DarcyTools version 3.4 – Concepts, methods and equations. SKB R-07-34, Svensk Kärnbränslehantering AB.

Öhman J, Bockgård N, Follin S, 2012. Site investigation SFR. Bedrock hydrogeology. SKB R-11-03, Svensk Kärnbränslehantering AB.

Unpublished documents

SKBdoc id, version	Title	Issuer, year
1395214 ver. 1.0	TD08- SFR3 affect on the performance of the existing SFR1	SKB, 2013
1395344 ver. 1.0	TD-05_JÖ	SKB, 2013